International Journal of Engineering Research and Science & Technology

www.ijerst.org

ISSN : 2319-5991

Vol. 21 No. 3 (1) 2025

ijerst.editor@gmail.com

editor@ijerst.com

ISSN 2319-5991 www.ijerst.com
Vol. 21, No. 3(1), 2025

Research Paper

ANALYSIS AND DESIGN OF STEEL SUPPORTING STRUCTURE FOR CHIMNEY

CHILUVERU RAVALIKA[1], T.SUJATHA[2]

[1]*M. Tech Student, Department of Civil Engineering, JNTUH University College of Engineering Sultanpur, Sultanpur, Choutkur, Telangana 502273*

[2]*Assistant professor, Department of Civil Engineering, JNTUH University College of Engineering Sultanpur, Sultanpur, Choutkur, Telangana 502273*

Abstract *Industries like power, cement, and chemical plants increasingly use tall chimneys for pollution control, which face strong wind and seismic forces, demanding stable and durable support systems. Steel Supporting structures are fundamental components in various industrial systems, especially for tall installations such as chimneys, towers and stacks. This study focuses on developing a safe, economical and efficient steel framework for chimney capable of withstanding gravity loads, wind loads and seismic loads as per the Indian standards. Conventional open sections such as Channel Sections and Angle sections are initially used in the model and then replaced with hollow sections to evaluate their structural efficiency and weight advantages and presents a comparative structural analysis of four distinct supporting frame models designed as a chimney support structure located in Bhuvaneswar, using STAAD.Pro as the primary analysis tool.*

The comparison of these four models illustrates the trade-offs between different steel section profiles in terms of structural weight, member efficiency, and potential fabrication complexity. CHS-based structures, though more complex in connection design, offer superior material savings and aesthetic advantages. The findings guide structural engineers in developing economical, efficient, and reliable chimney support systems with modern hollow steel sections. This study demonstrates the potential for material savings of up to 24% by transitioning from traditional ISMC to hollow steel sections, promoting sustainable and efficient structural design practices.

Keywords: *Chimney Support Structure, Wind Analysis, Seismic Analysis, Structural efficiency, Material Weight optimization*

Received: 14-08-2025 Accepted: 16-09-2025 Published: 23-09-2025

1. Introduction

In the field of structural engineering, the optimization of supporting frameworks for industrial infrastructure has garnered significant attention in recent decades. Chimney structures, particularly in thermal power plants, cement industries, and other heavy industrial installations, require stable and robust support systems that can withstand various environmental and operational loads over extended periods. These support structures are subjected to critical loading conditions such as wind loads, seismic activities, thermal expansion, and vibrations arising from chimney operations. Therefore, the design of an efficient, durable, and cost-effective supporting frame becomes a vital consideration for ensuring the safety and functionality of these essential components.

Traditionally, chimney support structures have been constructed using standard hot-rolled steel sections like Indian Standard Medium Channels (ISMC) and Indian Standard Angles (ISA), primarily due to their widespread availability, ease of fabrication, and well-established design methodologies. These conventional sections have served as the backbone of numerous structural applications for decades. However, with the rising cost of materials, growing concerns about sustainability, and the advancement of computational design tools, there has been a paradigm shift toward exploring alternative structural configurations that offer better material utilization without compromising safety or structural performance.

The emergence of hollow structural sections (HSS), particularly Rectangular Hollow Sections (RHS) and Circular Hollow Sections (CHS), has opened new avenues for structural designers. These modern steel profiles possess unique geometric and mechanical advantages. Unlike open sections, hollow sections exhibit higher torsional rigidity, better resistance to buckling, and improved aesthetic appeal. Furthermore, due to their closed form, they offer a reduced surface area exposed to environmental factors, which can potentially extend the lifespan of the structure by minimizing corrosion. In recent years, the structural efficiency of RHS and CHS members has led to their `widespread adoption in applications ranging from space frames and trusses to sign gantries and industrial support towers.

The integration of advanced analysis tools like STAAD.Pro has further revolutionized structural design practices. STAAD.Pro enables engineers to perform detailed finite element analysis (FEA) and structural simulations with a high degree of accuracy. Through its powerful modelling environment, it is possible to evaluate different structural configurations, member properties, and loading scenarios to arrive at an optimal design solution. This computational capability allows engineers to go beyond conventional design practices and explore more complex geometries and member combinations, including hybrid configurations involving multiple section types.

This paper builds upon these emerging practices by evaluating and comparing four different structural models of a chimney support system located in Bhubaneswar, India a region with moderate seismic activity and substantial wind loading considerations. The primary aim is to investigate how different steel member profiles influence the overall efficiency and weight of the supporting structure.

Model 1 represents the baseline design, constructed using standard ISMC and ISA sections, which are commonly employed in many existing industrial installations. This configuration provides a benchmark against which the other models can be assessed. While structurally sound, such designs may not be the most material-efficient, especially when evaluated in light of modern engineering standards that emphasize sustainability and resource optimization.

Model 2 introduces RHS members in place of ISMC profiles, aiming to capitalize on the improved structural performance of hollow rectangular sections. This change results in a notable reduction in structural steel weight—by approximately 15.5%—highlighting the potential for material savings through judicious member selection. RHS sections, due to their closed geometry, offer increased strength-to-weight ratios and reduced exposure to corrosion-prone surfaces, which can lead to long-term maintenance benefits.

Model 3 further enhances the structure by replacing ISA bracing members with CHS profiles, while retaining RHS for the main framing components. This hybrid model seeks to explore the advantages of combining two types of hollow sections, aiming to strike a balance between structural performance and ease of fabrication. Although the steel weight slightly increases due to the geometric characteristics of CHS members, this trade-off may be justified by potential improvements in durability, aesthetics, and torsional behavior.

Finally, Model 4 presents an entirely CHS-based configuration, utilizing circular sections for both primary and secondary members. This model achieves the lowest structural steel weight of all, amounting to a 24% reduction when compared with the traditional ISMC-ISA configuration of Model 1. Such a significant material saving not only reduces direct construction costs but also promotes sustainability by minimizing raw material consumption.

Despite potential complexities in connection detailing and fabrication associated with CHS members, their advantages in strength, durability, and appearance make them a compelling choice for modern structural applications. The comparative analysis of these four models is not merely academic; it reflects a broader shift in structural engineering practice toward more sustainable and cost-effective design strategies. With increasing emphasis on green building practices and life-cycle performance, engineers are now tasked with delivering solutions that minimize environmental impact without sacrificing safety or performance. This study contributes to that evolving body of knowledge by demonstrating how different structural steel profiles can be leveraged to optimize chimney support frames. Furthermore, this research underscores the importance of computational modelling in modern engineering workflows. Without tools like STAAD.Pro, conducting such a detailed comparative study accounting for numerous load combinations, structural behaviors, and member interactions would be time-consuming and error-prone.

The ability to simulate real-world conditions, apply iterative refinements, and extract performance metrics from multiple design variants empowers engineers to make informed design decisions grounded in quantitative analysis. The background of this study is rooted in the practical necessity of optimizing structural support systems for industrial chimneys. It is motivated by the desire to reduce material usage, improve structural efficiency, and incorporate modern steel profiles that align with contemporary engineering goals. Through a systematic evaluation of four distinct models, the study highlights the performance, trade-offs, and advantages of transitioning from traditional open sections to modern hollow sections. These insights have the potential to guide engineers, designers, and project stakeholders in adopting more efficient structural systems that align with both technical and environmental objectives.

1.1 Objectives of the study

The primary objective of this research is to perform a comprehensive comparative structural analysis of various chimney support frame configurations using different types of steel member sections, with a focus on optimizing the structure for material efficiency, structural integrity, and design economy. The study is centered around the structural modeling and analysis of four support frame models using STAAD.Pro, incorporating Indian Standard Medium Channels (ISMC), Angle Sections (ISA), Rectangular Hollow Sections (RHS), and Circular Hollow Sections (CHS).

The specific objectives of this thesis are outlined as follows:

1. To develop four distinct structural models of chimney support frames using different combinations of steel member sections—namely, ISMC with ISA (Model 1), RHS (Model 2), RHS with CHS (Model 3), and full CHS sections (Model 4).
2. To conduct structural analysis of each frame model using STAAD.Pro to evaluate key structural parameters such as axial force distribution, support reactions, and overall structural behavior under applied loads.
3. To quantify the total structural steel weight used in each configuration and assess the material efficiency achieved by substituting conventional sections with hollow sections (RHS and CHS).
4. To evaluate the trade-offs and challenges associated with using hollow sections practical constructability in comparison to traditional rolled sections.

By achieving the above objectives, this research aims to contribute meaningful knowledge to the field of structural engineering, particularly in optimizing industrial support structures. The outcomes are intended to serve as a reference for future design practices that prioritize sustainability, structural efficiency, and economic feasibility.

2. Literature Reviews

T Saran Kumar, R. Naga Vinothini (2015) presented the study of vortex shedding effect on steel chimney. Vortex shedding means at certain velocities air or fluid past a cylindrical body forms an oscillating flow, which depends on the size and shape of the body. Reynolds number used to predict fluid flow pattern fast a body is steady were turbulent. Five models of chimneys with different heights and diameters at top and bottom, were designed as per IS 6533 1989(part 2) and wind load was calculated as per IS 875 (part 3)-1987.The study on the vortex shedding effect on different chimney models reveals that the wind induced vibration in the tall chimneys varies with respect to height.

Haris et al. (2018) An Experimental Study of Bending Behavior of Double Channel and Hollo Sections of Light Gauge Steel Haris, Prasetio, Thamrin, and Herman (2018) compared the structural behavior of double channel open sections with hollow sections in light gauge steel under bending conditions. The experimental results revealed that hollow sections exhibited superior out-of-plane stability and more uniform stress distribution, while double channel sections were prone to lateral-torsional buckling. Both section types showed similar initial bending behavior, but hollow sections maintained their performance for longer before local buckling initiated. This study emphasized the enhanced stability and load-resisting capacity of hollow sections when subjected to flexural loading.

Aiyan et al (2024) investigated the use of lattice structural systems to mitigate the effects of vortex shedding on high-rise chimneys. Their study focused on optimizing the lattice bracing arrangements to reduce wind-induced oscillations and improve the dynamic stability of tall chimney structures. Using computational simulations, the authors demonstrated that properly designed lattice frameworks can significantly lower vortex- induced vibrations and enhance the overall structural resilience. This research highlights the importance of redundant support and lattice configurations as a practical measure for protecting slender vertical structures against aerodynamic instabilities, providing guidance for the design of tall industrial chimneys.

3. Research methodology

In this research, four different steel section types—Indian Standard Medium Channel (ISMC), Indian Standard Angle (ISA), Rectangular Hollow Section (RHS), and Circular Hollow Section (CHS)—are considered for the construction of chimney support frames. Each section type offers unique structural characteristics, and their comparative evaluation is necessary to determine the optimal choice for both strength and material economy. The research methodology ensures that these section types are analyzed under identical conditions to provide a fair and precise comparison. The study follows a simulation-driven research approach using STAAD.Pro, a widely recognized software for structural analysis and design. This tool enables accurate modeling of complex geometries, application of realistic loading conditions, and execution of advanced analysis methods as per relevant design codes such as IS 800:2007, IS 1893 and IS 875. The methodology also incorporates optimization strategies to fine-tune the section.

3.1 Research design

The research design for this study follows a comparative and simulation-based experimental approach, structured to ensure that the evaluation of chimney support frame structures is conducted in a methodical and reproducible

International Journal of Engineering Research and Science & Technology

manner. The framework is developed to systematically assess the performance of four steel section types ISMC, ISA, RHS, and CHS under identical loading and boundary conditions, thereby eliminating external variations that could bias the results. The overall research framework is divided into sequential stages: problem definition, model development, simulation and analysis, optimization, and comparative evaluation.

In the problem definition stage, the need for material optimization without compromising structural safety is clearly established. This sets the foundation for selecting chimney support structures as the focal application due to their critical role in industrial settings such as power plants, manufacturing facilities, and processing units. In the model development stage, detailed 3D models of the chimney support frames are created in STAAD. Pro. Each model incorporates the geometric dimensions, connection details, and material properties specific to the chosen steel section.

The modeling process adheres strictly to Indian design standards, including IS 800:2007 for steel design, IS 875 (Parts 1–3) for load calculations, and IS 1893 for seismic considerations. The simulation and analysis stage involves applying realistic loading conditions, including dead loads, live loads, wind loads, and seismic forces, as per the site-specific conditions considered in the study. STAAD. Pro is used to perform linear static analysis, wind load simulation, and seismic analysis, ensuring that each design is tested against both serviceability and ultimate limit states. Key performance indicators (KPIs) such as maximum displacement, axial force distribution, bending moments, and member stresses are extracted for further evaluation. The optimization stage employs a performance-based selection approach to determine the most suitable section type for the chimney support frame.

The primary optimization criterion is material usage minimization while ensuring compliance with safety limits. Secondary considerations include structural stiffness, stability, and cost implications. This approach ensures that the final selection balances engineering performance with economic feasibility. Finally, the comparative evaluation stage involves analyzing simulation results across all four section types. Performance metrics are compiled into a comparative matrix that highlights the trade-offs between different section geometries.

This structured evaluation framework enables the identification of the most efficient and practical steel section for chimney support structures. The research framework is visualized through a flowchart that illustrates the logical progression from problem identification to result interpretation. This structured design ensures transparency, reproducibility, and practical relevance, making it suitable for both academic and industry adoption.

3.2 Model Used in STAAD Pro Software

As per the assumed data for the structure the 3D model is made in STAAD software and then we applied the loads for the members and then analysis is made using wind load analysis and seismic load analysis. The generated 3d model of chimney supported tower is shown in the below figure.

Fig 1: 3d Rendered model

4. Results and analysis

The four models evaluated in this study differ primarily in the cross-sectional profiles of their main and bracing members:

Model 1 uses conventional Indian Standard Medium Channel (ISMC) sections for the main members and Indian Standard Angle (ISA) sections for bracings.

Model 2 replaces the ISMC sections with equivalent Rectangular Hollow Sections (RHS), aiming to reduce weight and improve section efficiency.

Model 3 further modifies the bracing members by replacing ISA sections with Circular Hollow Sections (CHS) while retaining RHS for main members, thus introducing torsional advantages while slightly increasing total weight.

Model 4 adopts CHS sections for both main and bracing members, targeting maximum material efficiency.

4.1 Model 1 Results

Table 1: Node Displacements results for model 1

Node Displacements						
			Horizontal	Vertical	Horizontal	Resultant
	Node	L/C	X mm	Y mm	Z mm	mm
Max X	114	20 0.9(DL)+1.5(WLX)	119.301	3.193	-0.299	119.344
Min X	114	21 0.9(DL)+1.5(-WLX)	-119.32	-3.775	0.306	119.38
Max Y	116	22 0.9(DL)+1.5(WLZ)	-0.556	4.251	156.254	156.313
Min Y	116	23 0.9(DL)+1.5(-WLZ)	0.537	-4.831	-156.247	156.322
Max Z	114	22 0.9(DL)+1.5(WLZ)	-0.327	-4.821	156.465	156.539
Min Z	114	23 0.9(DL)+1.5(-WLZ)	0.307	4.239	-156.458	156.516
Max rX	104	22 0.9(DL)+1.5(WLZ)	-0.5	4.216	121.447	121.521
Min rX	103	23 0.9(DL)+1.5(-WLZ)	0.292	4.217	-121.432	121.506
Max rY	92	22 0.9(DL)+1.5(WLZ)	-0.508	4.002	86.831	86.925
Min rY	92	23 0.9(DL)+1.5(-WLZ)	0.516	-4.51	-86.847	86.966
Max rZ	104	21 0.9(DL)+1.5(-WLX)	-92.528	3.169	0.358	92.583
Min rZ	101	20 0.9(DL)+1.5(WLX)	92.505	3.176	-0.276	92.56
Max R_u	114	22 0.9(DL)+1.5(WLZ)	-0.327	-4.821	156.465	156.539

Table 2: Beam End Forces results for model 1

	Beam	L/C	Node	Fx (KN)	Fy (KN)	Fz (KN)	Mx (KN.m)	My (KN.m)	Mz (KN.m)
Max Fx	16	0.9(DL)+1.5(WLZ)	13	337.475	-0.418	22.518	0	0	0
Min Fx	1	0.9(DL)+1.5(WLZ)	3	-302.944	0.301	22.109	0	13.912	-0.188
Max Fy	102	0.9(DL)+1.5(WLZ)	41	6.487	152.289	-5.381	0.028	0.897	0.024
Min Fy	104	0.9(DL)+1.5(WLZ)	43	7.57	-151.906	6.116	-0.028	1.015	0.024
Max Fz	16	0.9(DL)+1.5(WLZ)	13	337.475	-0.418	22.518	0	0	0
Min Fz	1	0.9(DL)+1.5(WLZ)	1	337.473	-0.418	-22.518	0	0	0
Max Mx	35	0.9(DL)+1.5(WLZ)	23	-1.8	68.31	-5.912	0.049	0.994	5.011
Min Mx	92	0.9(DL)+1.5(WLZ)	44	-2.84	-68.477	6.728	-0.049	-0.89	-15.516
Max My	16	0.9(DL)+1.5(WLZ)	15	337.223	-0.418	22.219	0	13.981	0.262
Min My	1	0.9(DL)+1.5(WLZ)	3	337.221	-0.418	-22.22	0	-13.981	0.262
Max Mz	102	0.9(DL)+1.5(WLZ)	49	-6.22	-140.84	5.121	-0.022	0.679	42.218
Min Mz	102	0.9(DL)+1.5(WLZ)	49	6.487	152.168	-5.381	0.028	-0.717	-45.645

Table 3: Support Reactions results for model 1

Support reactions					
			Horizontal	Vertical	Horizontal
	Node	L/C	Fx (KN)	Fy (KN)	Fz (KN)
Max Fx	13	0.9(DL)+1.5(-WLX)	16.832	259.791	0.24
Min Fx	14	0.9(DL)+1.5(WLX)	-16.832	259.789	0.241
Max Fy	13	0.9(DL)+1.5(-WLZ)	0.418	337.475	22.518
Min Fy	1	0.9(DL)+1.5(-WLZ)	-0.301	-302.692	22.408
Max Fz	13	0.9(DL)+1.5(-WLZ)	0.418	337.475	22.518
Min Fz	1	0.9(DL)+1.5(WLZ)	0.418	337.473	-22.518
Max Mx	1	1 EQ +X	-0.462	-10.847	0.011
Min Mx	1	1 EQ +X	-0.462	-10.847	0.011
Max My	1	1 EQ +X	-0.462	-10.847	0.011
Min My	1	1 EQ +X	-0.462	-10.847	0.011
Max Mz	1	1 EQ +X	-0.462	-10.847	0.011
Min Mz	1	1 EQ +X	-0.462	-10.847	0.011

4.2 Model 2 Results

Table 4: Node Displacements results for model 2

NODE DISPLACEMENTS									
			Horizontal	Vertical	Horizontal	Resultant	Rotational		
	Node	L/C	X mm	Y mm	Z mm	mm	rX rad	rY rad	rZ rad
Max X	114	0.9(DL)+1.5(WLX)	143.302	4.126	-0.443	143.363	0	0	-0.007
Min X	114	0.9(DL)+1.5(WLX)	-143.31	-4.739	0.429	143.389	0	0	0.007
Max Y	116	0.9(DL)+1.5(WLZ)	-0.786	5.123	176.086	176.163	0.009	0	0
Min Y	116	0.9(DL)+1.5(WLZ)	0.779	-5.734	-176.1	176.195	-0.009	0	0
Max Z	114	0.9(DL)+1.5(WLZ)	-0.474	-5.697	176.381	176.473	0.009	0	0
Min Z	114	0.9(DL)+1.5(WLZ)	0.466	5.084	-176.395	176.468	-0.009	0	0
Max rX	109	0.9(DL)+1.5(WLZ)	-0.766	5.107	162.653	162.735	0.009	0	0
Min rX	107	0.9(DL)+1.5(WLZ)	0.425	5.06	-148.549	148.635	-0.009	0	0
Max rY	84	0.9(DL)+1.5(WLZ)	-0.725	4.104	69.364	69.489	0.007	0	0
Min rY	84	0.9(DL)+1.5(WLZ)	0.757	-4.545	-69.41	69.562	-0.007	0	0
Max rZ	104	0.9(DL)+1.5(WLX)	-109.185	4.094	0.541	109.263	0	0	0.007
Min rZ	105	0.9(DL)+1.5(WLX)	120.551	4.104	-0.6	120.621	0	0	-0.007
Max Rst	113	0.9(DL)+1.5(WLZ)	0.778	-5.723	-176.392	176.486	-0.009	0	0

Table 5: Beam End Forces results for model 2

BEAM END FORCES									
	Beam	L/C	Node	Fx (KN)	Fy (KN)	Fz (KN)	Mx (KN.m)	My (KN.m)	Mz (KN.m)
Max Fx	16	0.9(DL)+1.5(WLZ)	13	336.135	-0.404	22.511	0	0	0
Min Fx	1	0.9(DL)+1.5(WLZ)	3	-304.459	0.296	22.121	0	13.919	-0.185
Max Fy	102	0.9(DL)+1.5(WLZ)	41	6.313	144.295	-5.658	1.662	0.943	2.254
Min Fy	104	0.9(DL)+1.5(WLZ)	43	7.459	-144.031	6.542	-1.645	1.081	2.251
Max Fz	16	0.9(DL)+1.5(WLZ)	13	336.135	-0.404	22.511	0	0	0
Min Fz	1	0.9(DL)+1.5(WLZ)	1	336.133	-0.404	-22.511	0	0	0
Max Mx	74	0.9(DL)+1.5(WLZ)	36	-13.416	31.062	0.757	4.026	0.025	0.217
Min Mx	74	0.9(DL)+1.5(WLZ)	36	13.756	-26.422	-0.756	-4.024	-0.028	0.216
Max My	16	0.9(DL)+1.5(WLZ)	15	335.888	-0.404	22.213	0	13.976	0.252
Min My	1	0.9(DL)+1.5(WLZ)	3	335.885	-0.404	-22.213	0	-13.976	0.253
Max Mz	102	0.9(DL)+1.5(WLZ)	49	-6.123	-134.123	5.474	-1.538	0.727	38.441
Min Mz	102	0.9(DL)+1.5(WLZ)	49	6.313	144.177	-5.658	1.662	-0.754	-41.017

Table 6: Support Reactions results for model 2

SUPPORT REACTIONS					
			Horizontal	Vertical	Horizontal
	Node	L/C	Fx (KN)	Fy (KN)	Fz (KN)
Max Fx	13	0.9(DL)+1.5(-WLX)	18.194	276.394	0.192
Min Fx	14	0.9(DL)+1.5(WLX)	-18.194	276.391	0.192
Max Fy	13	0.9(DL)+1.5(-WLZ)	0.404	336.135	22.511
Min Fy	1	0.9(DL)+1.5(-WLZ)	-0.296	-304.211	22.42
Max Fz	13	0.9(DL)+1.5(-WLZ)	0.404	336.135	22.511
Min Fz	1	0.9(DL)+1.5(WLZ)	0.404	336.133	-22.511
Max Mx	1	EQ +X	-0.418	-9.682	0.007
Min Mx	1	EQ +X	-0.418	-9.682	0.007
Max My	1	EQ +X	-0.418	-9.682	0.007
Min My	1	EQ +X	-0.418	-9.682	0.007
Max Mz	1	EQ +X	-0.418	-9.682	0.007
Min Mz	1	EQ +X	-0.418	-9.682	0.007

4.3 Model 3 Results

Table 7: Node Displacements results for model 3

NODE DISPLACEMENTS						
			Horizontal	Vertical	Horizontal	Resultant
	Node	L/C	X mm	Y mm	Z mm	mm
Max X	114	0.9(DL)+1.5(WLX)	136.855	3.93	-0.42	136.912
Min X	114	0.9(DL)+1.5(-WLX)	-136.862	-4.56	0.405	136.939
Max Y	116	0.9(DL)+1.5(WLZ)	-0.768	4.929	169.477	169.551
Min Y	116	0.9(DL)+1.5(-WLZ)	0.761	-5.556	-169.492	169.585
Max Z	114	0.9(DL)+1.5(WLZ)	-0.458	-5.519	169.771	169.861
Min Z	114	0.9(DL)+1.5(-WLZ)	0.451	4.89	-169.786	169.857
Max rX	112	0.9(DL)+1.5(WLZ)	-0.748	4.924	156.204	156.283
Min rX	107	0.9(DL)+1.5(-WLZ)	0.41	4.867	-142.906	142.99
Max rY	84	0.9(DL)+1.5(WLZ)	-0.707	3.956	66.716	66.837
Min rY	84	0.9(DL)+1.5(-WLZ)	0.741	-4.407	-66.765	66.914
Max rZ	108	0.9(DL)+1.5(-WLX)	-115.057	3.941	0.585	115.126
Min rZ	105	0.9(DL)+1.5(WLX)	115.068	3.91	-0.378	115.135
Max Rst	113	0.9(DL)+1.5(-WLZ)	0.76	-5.545	-169.783	169.875

Table 8: Beam end forces results for model 3

BEAM END FORCES									
	Beam	L/C	Node	Fx (KN)	Fy (KN)	Fz (KN)	Mx KN.m)	My KN.m)	Mz KN.m)
Max Fx	16	0.9(DL)+1.5(-WLZ)	13	328.607	-0.404	22.151	0	0	0
MinFx	1	0.9(DL)+1.5(-WLZ)	3	296.551	0.295	21.759	0	13.693	-0.184
Max Fy	103	0.9(DL)+1.5(-WLZ)	41	6.187	140.59	-6.586	1.676	0.932	2.229
Min Fy	104	0.9(DL)+1.5(WLZ)	43	7.3	-140.33	6.449	-1.659	1.066	2.226
Max Fz	16	0.9(DL)+1.5(-WLZ)	13	328.607	-0.404	22.151	0	0	0
Min Fz	1	0.9(DL)+1.5(WLZ)	1	328.604	-0.405	-22.151	0	0	0
ax Mx	74	0.9(DL)+1.5(WLZ)	36	-13.197	38.27	0.767	3.89	0.024	0.343
Min Mx	74	0.9(DL)+1.5(-WLZ)	36	13.834	-25.468	-0.767	-3.888	-0.027	0.241
Max My	16	0.9(DL)+1.5(-WLZ)	14	328.36	-0.404	21.852	0	13.781	0.253
Min My	1	0.9(DL)+1.5(WLZ)	3	328.387	-0.405	-21.852	0	-13.781	0.253
Max Mz	103	0.9(DL)+1.5(WLZ)	49	-6.984	-138.2	6.399	-1.338	0.716	37.383
Min Mz	103	0.9(DL)+1.5(-WLZ)	49	6.187	140.472	-6.586	1.676	-0.744	-39.931

Table 9: Support Reactions results for model 3

SUPPORT REACTIONS					
			Horizontal	Vertical	Horizontal
	Node	L/C	Fx KN	Fy KN	Fz KN
Max Fx	13	21 0.9(DL)+1.5(-WLX)	17.832	268.931	0.192
Min Fx	14	20 0.9(DL)+1.5(WLX)	-17.832	268.928	0.192
Max Fy	13	23 0.9(DL)+1.5(-WLZ)	0.404	328.607	22.151
Min Fy	1	23 0.9(DL)+1.5(-WLZ)	-0.295	-296.103	22.058
Max Fz	13	23 0.9(DL)+1.5(-WLZ)	0.404	328.607	22.151
Min Fz	1	22 0.9(DL)+1.5(WLZ)	0.405	328.604	-22.151
Max Mx	1	1 EQ +X	-0.427	-9.922	0.008
Min Mx	1	1 EQ +X	-0.427	-9.922	0.008
Max My	1	1 EQ +X	-0.427	-9.922	0.008
Min My	1	1 EQ +X	-0.427	-9.922	0.008
Max Mz	1	1 EQ +X	-0.427	-9.922	0.008
Min Mz	1	1 EQ +X	-0.427	-9.922	0.008

4.4 MODEL 4

Table 10: Node Displacements results for model 4

NODE DISPLACEMENTS						
			Horizontal	Vertical	Horizontal	Resultant
	Node	L/C	X mm	Y mm	Z mm	mm
Max X	114	0.9(DL)+1.5(WLX)	232.552	6.476	-0.525	232.642
Min X	114	0.9(DL)+1.5(-WLX)	-232.577	-7.284	0.551	232.692
Max Y	116	0.9(DL)+1.5(-WLX)	-232.381	6.48	0.81	232.472
Min Y	114	0.9(DL)+1.5(-WLX)	-232.577	-7.284	0.551	232.692
Max Z	114	0.9(DL)+1.5(WLZ)	-0.501	-7.263	231.958	232.072
Min Z	114	0.9(DL)+1.5(-WLZ)	0.476	6.455	-231.932	232.023
Max rX	112	0.9(DL)+1.5(WLZ)	-0.816	6.454	214.225	214.324
Min rX	107	0.9(DL)+1.5(-WLZ)	0.438	6.434	-196.748	196.853
Max rY	92	0.9(DL)+1.5(WLZ)	-0.758	6.101	127.646	127.794
Min rY	92	0.9(DL)+1.5(-WLZ)	0.772	-6.805	-127.66	127.843
Max rZ	108	0.9(DL)+1.5(-WLX)	-197.384	6.473	0.772	197.491
Min rZ	105	0.9(DL)+1.5(WLX)	197.38	6.454	-0.484	197.486
Max Rst	**114**	**0.9(DL)+1.5(-WLX)**	**-232.577**	**-7.284**	**0.551**	232.692

Table 11: Beam end forces results for model 4

BEAM END FORCES									
	Beam	L/C	Node	Fx (KN)	Fy (KN)	Fz (KN)	Mx (KN.m)	My (KN.m)	Mz (KN.m)
Max Fx	3	0.9(DL)+1.5(WLX)	2	299.779	19.07	0.186	0	0	0
Min Fx	1	0.9(DL)+1.5(WLX)	3	-271.731	18.805	0.13	0	0.081	-11.818
Max Fy	103	0.9(DL)+1.5(WLX)	44	6.554	130.17	-3.584	3.079	0.937	4.702
Min Fy	106	0.9(DL)+1.5(WLX)	46	5.732	-130.137	4.93	-3.08	0.837	4.689
Max Fz	16	0.9(DL)+1.5(WLZ)	13	299.049	-0.137	19.081	0	0	0
Min Fz	1	0.9(DL)+1.5(WLZ)	1	299.046	-0.137	-19.081	0	0	0
Max Mx	50	0.9(DL)+1.5(WLX)	28	-4.829	25.66	0.668	6.33	-0.022	0.487
Min Mx	50	0.9(DL)+1.5(WLX)	28	5.416	-20.954	-0.668	-6.334	0.021	0.497
Max My	16	0.9(DL)+1.5(WLZ)	15	298.869	-0.137	18.872	0	11.86	0.086
Min My	117	0.9(DL)+1.5(WLZ)	49	260.679	-2.836	-7.631	0.203	-12	3.325
Max Mz	106	0.9(DL)+1.5(WLX)	51	-5.477	120.465	-4.709	2.511	0.621	32.18
Min Mz	106	0.9(DL)+1.5(WLX)	51	5.732	-130.251	4.93	-3.08	-0.642	-34.399

Table 12: Support Reactions results for model 4

SUPPORT REACTIONS					
			Horizontal	Vertical	Horizontal
	Node	L/C	Fx (KN)	Fy (KN)	Fz (KN)
Max Fx	13	0.9(DL)+1.5(-WLX)	19.14	299.206	0.063
Min Fx	14	0.9(DL)+1.5(WLX)	-19.14	299.203	0.063
Max Fy	2	0.9(DL)+1.5(WLX)	-19.07	299.779	-0.186
Min Fy	1	0.9(DL)+1.5(WLX)	-19.013	-271.551	0.13
Max Fz	13	0.9(DL)+1.5(-WLZ)	0.137	299.049	19.081
Min Fz	1	0.9(DL)+1.5(WLZ)	0.137	299.046	-19.081
Max Mx	1	EQ +X	-0.362	-8.586	0.003
Min Mx	1	EQ +X	-0.362	-8.586	0.003
Max My	1	EQ +X	-0.362	-8.586	0.003
Min My	1	EQ +X	-0.362	-8.586	0.003
Max Mz	1	EQ +X	-0.362	-8.586	0.003
Min Mz	1	EQ +X	-0.362	-8.586	0.003

4.5 Shear Force Comparison

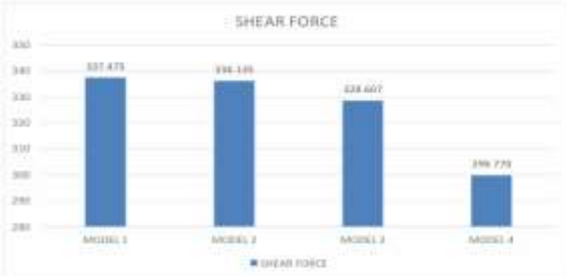

Graph 1: Comparison of Shear Force

4.6 Bending moment

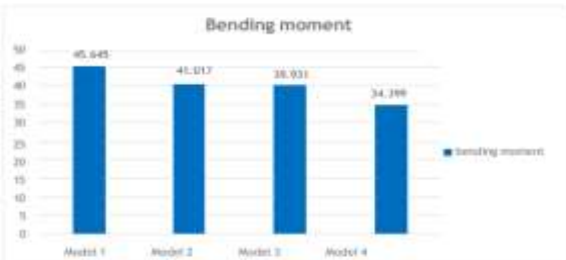

Graph 2: Comparison of Bending moment

4.7 Axial force

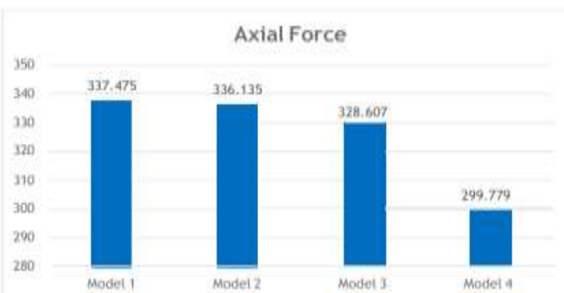

4.8 Comparison of Axial Force

Graph 3: Comparisons of Node Displacements

4.9 Beam Relative Displacements

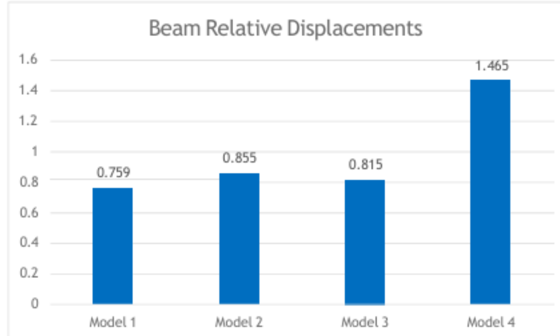

Graph 4: Comparison of Beam Relative Displacements

4.10 Discussions

The comparative structural analysis of the four chimney support frame models—Model 1 (ISMC + ISA), Model 2 (RHS replacing ISMC), Model 3 (RHS + CHS replacing ISA), and Model 4 (full CHS)—reveals significant insights into structural efficiency, material usage, and overall performance. Each model was assessed under identical loading conditions using STAAD.Pro, with particular emphasis on beam end forces, node displacements, support reactions, and static check results.

One of the primary observations is the substantial reduction in structural steel weight as the design transitions from conventional rolled sections (ISMC and ISA) to hollow sections (RHS and CHS). Model 1, utilizing standard ISMC and ISA members, had the highest steel weight, indicating a less material-efficient design. Replacing ISMC members with RHS in Model 2 reduced the weight by approximately 15%, reflecting the superior strength-to- weight ratio of hollow sections.

Model 3's introduction of CHS members in place of ISA sections, while retaining RHS for main frames, resulted in a slight increase in weight compared to Model 2. This increase is attributed to the circular geometry of CHS, which typically uses more material per unit length than RHS but offers other performance benefits. Model 4, designed entirely with CHS members for both main and bracing elements, achieved the lowest steel weight overall a reduction of approximately 24% from Model 1 demonstrating the highest material efficiency.

Across all models, beam end forces and support reactions remained within safe limits, confirming structural adequacy. However, CHS-based models (Model 3 and Model 4) exhibited improved distribution of forces and moments, especially in torsional and bending components. The circular cross-section of CHS inherently provides uniform resistance to torsion and bending in multiple directions, unlike ISMC, ISA, or RHS sections, which have directional stiffness properties. For example, the maximum bending moments (Mx, My, Mz) and axial forces (Fx) in Model 4 were efficiently resisted with less material, showcasing the high structural efficiency of CHS. This characteristic is especially beneficial for chimney supports exposed to multidirectional wind loads and dynamic effects, where torsional rigidity is critical. Node displacement analysis revealed that all models-maintained displacements within acceptable serviceability limits.

However, Model 4 showed marginally higher displacements, consistent with its lighter steel weight, but these displacements were well within allowable limits, indicating no compromise in structural stability. The circular geometry of CHS not only provides torsional advantages but also contributes to better energy dissipation under dynamic loads, potentially enhancing durability under fluctuating wind and seismic conditions. While CHS offers multiple structural advantages, the fabrication and connection complexity must be acknowledged. Connections for CHS members require specialized detailing due to the curved surfaces, which can lead to increased fabrication costs and labor time compared to flat faced ISMC, ISA, or RHS sections.

Despite this, the long-term benefits in material savings, structural performance, and aesthetic appeal often outweigh the initial complexity. The significant material reduction up to 24% in Model 4 translates into lower raw material consumption, reduced transportation weight, and less embodied energy, making CHS-based designs more sustainable. This aligns with modern structural engineering trends prioritizing environmental responsibility without sacrificing performance.

Furthermore, lower material usage can lead to cost savings despite potentially higher fabrication expenses. The improved lifespan and maintenance benefits associated with CHS's superior corrosion resistance and durability further enhance the economic viability of such designs. Circular Hollow Sections (CHS) outperform traditional steel sections and RHS in chimney support structures primarily due to their:

Superior Torsional Resistance: CHS's uniform cross-section resists twisting forces more effectively, critical for tall slender structures like chimneys subjected to wind and seismic loads.

Material Efficiency: Despite slightly higher unit weights compared to RHS, CHS allows overall reduction in steel quantity while meeting strength and stiffness requirements.

Enhanced Aesthetic Appeal: CHS provide a clean, streamlined look preferred in modern architectural and industrial designs. Improved

Durability: CHS have fewer stress concentrations and better corrosion resistance, leading to longer service life. Sustainability: Material savings contribute to lower environmental impact and support green engineering practices. While the fabrication complexity and connection detailing for CHS are higher, the balance of performance benefits, sustainability, and cost-effectiveness makes CHS the optimal choice for chimney support frames. Model 4's superior results validate this conclusion, encouraging the adoption of full CHS frameworks in future chimney.

5. Conclusions

The primary objective of this thesis was to investigate and compare the structural performance, efficiency, and material optimization of four distinct chimney support frame configurations using STAAD.Pro, with a particular emphasis on the choice of steel member cross-sections. Each model employed a unique combination of Indian Standard Medium Channels (ISMC), Indian Standard Angles (ISA), Rectangular Hollow Sections (RHS), and Circular Hollow Sections (CHS) for the main framing and bracing members. The comparative analysis across the models has yielded critical insights into the relationship between member geometry, load distribution efficiency, and overall structural performance.

Model 1 served as the baseline configuration, incorporating ISMC members for the main framing and ISA sections for the bracing elements. This design represented a conventional approach to chimney support framing, widely used in industry due to its familiarity, ease of fabrication, and relatively low initial cost. While structurally adequate, the static check results revealed that the open-section ISMC and ISA members presented higher bending stresses and potential for localized buckling under certain load cases. Although the model exhibited perfect equilibrium in the static checks (zero differences between applied loads and reactions), the structural weight was comparatively higher, and the open-section geometry was less efficient in resisting torsional effects, especially under wind loading scenarios common to chimney structures.

Model 2 introduced a significant change by replacing ISMC main members with RHS sections, while retaining ISA for the bracing. RHS members, being closed sections, provided superior torsional rigidity and better resistance to biaxial bending compared to ISMC. This change resulted in improved structural stiffness and reduced susceptibility to local buckling. The static check results again confirmed perfect equilibrium, indicating sound load transfer and structural modeling. The increased performance, however, came with a marginal increase in fabrication complexity, as hollow sections require different connection detailing and often more precise cutting and welding compared to open channels. The ISA bracing still posed certain limitations in terms of torsional performance, leaving room for further optimization.

Model 3 pursued this optimization by replacing the ISA bracing in Model 2 with CHS members while retaining RHS for the main framing. This strategic substitution aimed to take advantage of CHS's isotropic properties, which provide uniform strength in all radial directions, superior buckling resistance, and better aerodynamic performance under wind loads. The static check results for Model 3 demonstrated perfect load-reaction balance, similar to the previous models, but the performance improvements were noticeable in the reduced maximum member forces and improved load distribution patterns. The bracing system, now consisting of CHS, exhibited enhanced capacity to carry compression loads without premature buckling, even under combined loading conditions. Additionally, the smooth outer surface of CHS bracing members offered reduced drag coefficient values, which can be particularly beneficial in chimney structures where wind loads are a critical design factor. Model 4 represented the most structurally efficient configuration by employing CHS members for both the main framing and the bracing elements. This design fully leveraged the mechanical and aerodynamic advantages of circular hollow profiles. The static check results confirmed equilibrium in all load cases, validating the accuracy of the load transfer paths. Compared to the previous configurations,

Model 4 achieved the lowest structural steel consumption without compromising stability or strength. The uniform distribution of stresses within CHS members allowed for a more efficient use of material, reducing member sizes and overall structural weight. The improved torsional stiffness minimized distortion under eccentric loads, while the closed geometry enhanced resistance against local buckling, making the frame highly resilient under dynamic and lateral load conditions such as wind gusts or seismic activity.

When comparing across the four models, it becomes evident that CHS sections consistently outperform open and rectangular hollow sections in key structural performance parameters. The primary reasons for this superiority are as follows:

Isotropic Strength Distribution – Unlike open sections (ISMC, ISA) or even rectangular sections (RHS) that have directional strength properties, CHS offers uniform resistance in all radial directions. This characteristic is particularly advantageous in chimney support frames, where members are subjected to complex load combinations from multiple directions. Superior Torsional

Rigidity – CHS profiles exhibit the highest torsional stiffness among common steel sections, which is critical for resisting twisting forces induced by wind or asymmetric loads on the chimney structure.

Enhanced Buckling Resistance – The closed circular geometry provides an optimal distribution of material around the centroid increasing the radius of gyration and thereby improving buckling resistance under compression. This allows for longer unsupported lengths and smaller cross-section sizes without sacrificing stability.

Aerodynamic Advantage – The circular profile reduces wind drag and vortex shedding effects compared to flat or angular profiles. This results in reduced dynamic wind load impact, which directly benefits fatigue life and serviceability performance.

Material Efficiency – CHS members utilize material more effectively by placing it farther from the centroid, maximizing the section modulus and minimizing unnecessary mass. This leads to a lighter structure, which in turn reduces foundation loads and potentially lowers construction costs.

Improved Aesthetics and Durability – Although secondary to structural concerns, the smooth and continuous surface of CHS members offers a more streamlined appearance and minimizes corrosion-prone crevices, enhancing durability in outdoor industrial environments.

References

1. Vakylabad, A. B., & Moravvej, Z. (2023). Environmental challenges of gases vent from flares and chimneys. In Crises in Oil, Gas and Petrochemical Industries (pp. 307-333). Elsevier.
2. Banerjee, S., Chatterjee, S., & Bhattacharya, K. (2012). Behavior of braced steel frames under wind and seismic loading. International Journal of Civil and Structural Engineering.
3. Giri, R., & Deb, S. K. (2005). Effectiveness of helical strakes in suppressing wind-induced oscillations in tall chimneys. Journal of Wind Engineering and Industrial Aerodynamics.
4. Gupta, A. K., & Gupta, M. S. (2004). Analysis and design of steel braced frames under lateral loads. Journal of Structural Engineering (India Saiyan, S., Shelepina, V., Yanushko, & Suleimanov, N. (2024). Application of lattice constructions for protection of high-rise chimneys from vortex shedding. E3S Web of Conferences, 533, 03003.
5. Simiu, E., & Scanlan, R. H. (1996). Wind effects on structures: Fundamentals and applications to design (3rd ed.). John Wiley & Sons.

6. Rajkumar, V., & Patil, B. (2013). Analysis of Self-Supporting Chimney. International Journal of Innovative Technology and Exploring Engineering, 3.
7. Birdean, C. I., & Cernescu, A. (2024). The mechanical performance of hidden in-line connection for hollow sections (Doctoral dissertation, Politehnica University Timișoara, Faculty of Mechanics).
8. Chavan, V. B., Nimbalkar, V. N., & Jasiwal, A. P. (2014). Economic evaluation of open and hollow structural sections in industrial trusses. International journal of innovative research in science, Engineering and technology, 3(2), 9554-9565.
9. Subramani, T., & Shanmugam, P. (2012). Seismic analysis and design of industrial chimneys by using staad pro. International Journal of Engineering Research and Applications (IJERA), ISSN, 2248-9622.
10. Liu, X. C., Yang, Z. W., Wang, H. X., Zhang, A. L., Pu, S. H., Chai, S. T., & Wu, L. (2017). Seismic performance of H-section beams to HSS column connection in prefabricated structures. Journal of constructional steel research, 138, 1-16.
11. Chavan, V. B., Nimbalkar, V. N., & Jasiwal, A. P. (2014). Economic evaluation of open and hollow structural sections in industrial trusses. International journal of innovative research in science, Engineering and technology, 3(2), 9554-9565.
12. Khalaf, M. S., Ibrahim, A. M., Najm, H. M., Sabri, M. M. S., Morkhade, S., Agarwal, A., ... & Alarifi, I. M. (2022). Experimental analysis of steel circular hollow section under bending loads: Comprehensive study of mechanical performance. Materials, 15(12), 4350. Grauvilardell, J. E., Lee, D., Hajjar, J. F., & Dexter, R. J. (2005). Synthesis of design, testing and analysis research on steel column base plate connections in high-seismic zones. Structural engineering report no. ST-04-02. Minneapolis (MN): Department of Civil Engineering, University of Minnesota.
13. Nuñez, E., Torres, R., & Herrera, R. (2017). Seismic performance of moment connections in steel moment frames with HSS columns. Steel Compos. Struct, 25(3), 271-286.
14. Birdean, C. I., & Cernescu, A. (2024). The mechanical performance of hidden in-line connection for hollow sections (Doctoral dissertation, Politehnica University Timișoara, Faculty of Mechanics).
15. Ammons, M. (2020). Enhancing Steel Hollow Structural Sections and Braced Frame Performance through Non-Traditional Civil Engineering Materials (Doctoral dissertation).
16. Chandna, H., Rampal, A., Bhardwaj, S., & Dhiman, A. (2015). Optimum Design of Transmission Towers using STAAD pro with Joints and Foundation Design in MS Excel VBA.